The Role of Cyanides and Isocyanides in Emissions Formation of Laminar Premixed Ammonia/Methane Flames

KOVALEVA, Marina[1]*, HAYAKAWA, Akihiro[2],OKAFOR, Ekenechukwu C[3], YAMASHITA, Hirofumi[2, 4], ALNASIF, Ali[1], VALERA-MEDINA, Agustin[1]
CRAYFORD, Andrew[1]

[1]*College of Physical Sciences and Engineering, Cardiff University, Cardiff CF24 3AA,Uited Kingdom*
[2]*Instituteof Fluid Science, Tohoku University, 2-1-1 Katahira, Aoba-ku, Sendai, Miyagi 980-8577 Japan*
[3]*Faculty of Engineering, Kyushu University, 744 Motooka, Nishi-ku, Fukuoka, 819-03965, Japan*
[4]*Department of Aerospace Engineering, Tohoku University, 6-6-01 Aramaki Aza Aoba, Aoba-ku, Sendai, Miyagi 980-8579, Japan*

Absract: As an intermediate step towards a low-carbon economy, blending of ammonia and fossil fuels in combustion devices are of interest as a method of CO_2 emissions reduction. However, compared to pure ammonia, NH_3/CH_4 blends produce higher peak NO emissions. C-N reactions have rarely been noted to be significant in most NOx emissions studies of NH_3/CH_4 blends and are excluded from many major ammonia mechanisms. This study uses emission data of NO, HCN, HNCO species in a one-dimensional, laminar, premixed burner-stabilized stagnation flame configuration to explore the contribution of these pathways to NO through the CEU-NH_3 (Wang) mechanism. This study highlights that rarely included hydrocarbon-nitrogen interactions contributed to 12.4% of NO formation in rich, ammonia heat ratio of 20% blends of NH_3/CH_4. Despite this, reactions with the highest contribution to the O, H, OH radical pool remain the controlling factor for NO formation.

Keywords : HNCO, HCNO, HCN, ammonia energy, emissions

1. Introduction

As an intermediate step towards a low-carbon economy, fossil fuel blends doped with ammonia are of interest as a method of CO_2 emissions reduction, however other harmful pollutants remain a challenge. Previous work shows that compared to NH_3/air flames, the addition of methane in ammonia/air flames increases peak NO production [1] and introduces CO, HCN emissions under rich conditions [2], which need to be predicted accurately. Therefore, accurate reaction chemistry models must be developed for these blends.

Recent studies report that across a range of equivalence ratios and blends, hydrocarbon-nitrogen interactions play a negligible role in NOx formation of NH_3/CH_4 flames. Like NH_3/H_2 blends, NO production is dominated by fuel-N routes (mostly through HNO, and to a smaller extent also through amines). Secondary sources of formation include through Zel'dovich and NO_2 reactions, meanwhile NO reduction takes place through Zel'dovich and amine routes [3]. These conclusions are based on literature analyzing NOx formation using Okafor [1, 4, 5], San Diego [4] , Sun et al. [6] and Konnov [7, 8] mechanisms. However, as Table 1 indicates, most of these mechanisms do not include detailed hydrocarbon-nitrogen chemistry. In contrast other studies that focus on nitrogen-bound fuels like coal [9], biomass [10], hydrocarbon with SCR through ammonia [11, 12], suggest that these nitrogen-hydrocarbon interactions are important in NOx formation. In studies of methane diluted with nitrogen, significant prompt-NO formation via HCN [13], and NCN [13] have been reported under rich conditions. NO-reburn, involving the reaction of hydrocarbon molecules with NO was found to be significant in syngas/CH_4 blends in a N_2 atmosphere [14]. These reactions either reduced NO to NH_x and N_2 ($NO \rightarrow HNCO \rightarrow NH_2 \rightarrow NNH \rightarrow N_2$) or to isocyanide/cyanide species ($NO \rightarrow HCN \rightarrow HNC \rightarrow HNCO$). Alternative NO consumption pathways to N_2 also include formation of HCNO or H_2CN molecules.

Therefore, this work aims to quantify the significance of prompt-NO, NO-reburn, methylamine and methyleneamine, hydrocarbon-amine interactions and other NCN and CH_x radical pool contributing reactions in the prediction of NH_3/CH_4 emissions. Experimental data [1] is utilized alongside a chemical reaction pathway analysis, to understand the contribution of these alternative reaction routes to the formation of NO.

Table 1. Comparison of hydrocarbon-ammonia chemistry in mechanisms [5, 6, 13, 16–18, 21–25]

		prompt-NO reactions				NO reburn via CHx + NO				$CH_x + NH_x$ reactions	
Mech.		NCN	HNCN	CN	HCN	NCO	H_2CN	HCNO	HNCO	CHxCN	CHxNHx
San Diego + full N chemistry (2018) [19]		×	×	×	×	×	×	×	×	×	×
Mei et al. (2021) [20]		×	×	×	×	×	×	×	×	×	×
Sun et al. (2022) [6]		×	×	✓	✓	✓	✓	✓	✓	×	×
GRI-3.0 [21]		×	×	✓	✓	✓	✓	✓	✓	×	×
Okafor et al. (2017) [5]		×	×	✓	✓	✓	✓	✓	✓	×	×
Shrestha et al. (2020) [22]		✓	✓	✓	✓	✓	✓	✓	✓	×	×
CEU-NH3 (Wang), (2020) [16]		✓	✓	✓	✓	✓	✓	✓	✓	×	×
Konnov et al. (2009) [13]		✓	✓	✓	✓	✓	✓	✓	✓	×	×
Glarborg et al. (2017) [23]		✓	✓	✓	✓	✓	✓	✓	✓	✓	✓
Arunthanayothin et al. (2021) [24]		✓	✓	✓	✓	✓	✓	✓	✓	✓	✓
POLIMI (2020) [25]		✓	✓	✓	✓	✓	✓	✓	✓	✓	✓

2. Methodology

For the numerical simulation, the Impinging Jet flame model of Cantera 2.6.0 [15] was employed. The curve and slope were set to 0.014 and 0.028 to ensure all simulations have ~800 grid points. Diffusion transport was calculated by a multi-component model with the Soret effect enabled. The NH_3/CH_4 fuel mixture was defined by an ammonia heat ratio, E_{NH3}, given by Eq. (1):

$$E_{NH3} = \frac{X_{NH3} \cdot LHV_{NH3}}{X_{NH3} \cdot LHV_{NH3} + X_{CH4} \cdot LHV_{CH4}} \quad (1)$$

Where LHV is the lower heating value of the fuels (LHV_{CH4} = 802.30 kJ/mol, LHV_{NH3} = 316.84 kJ/mol).

Figures 2, 5 and 6 show the variation of the integral value of the reaction R. Here, the value of I_R (in kmol/m^2/s) was calculated using Eq. (2), where L is the distance between the burner nozzle outlet and the stagnation plate, set to 20 mm:

$$I_R = \int_0^L \dot{\omega}_R \, dx \quad (2)$$

For modelling the experimental data, mechanisms with variation in the detail of hydrocarbon-nitrogen subsets were used. The CEU-NH_3 model by Wang et al. [16] with detailed hydrocarbon-nitrogen reaction subsets were selected and utilized for the analysis. Meanwhile, GRI-3.0 [17] and Okafor [5] mechanisms were selected as intermediate sized mechanisms and finally, UCSD (San Diego) [18] was selected as a mechanism with no significant hydrocarbon-nitrogen chemistry subsets.

3. Results and Discussion

Figure 1 shows the comparison between experimental and numerical NO prediction. As can be seen, with the exception of GRI-3.0 and UCSD, the mechanisms are generally able to predict NO emissions in the lean region, however they all underpredict the empirical NO emissions at rich conditions, with the POLIMI and Wang mechanisms offering best agreement. Whether this is due to their detailed nitrogen-hydrocarbon chemistry, relevant to NOx formation in the rich region is investigated further.

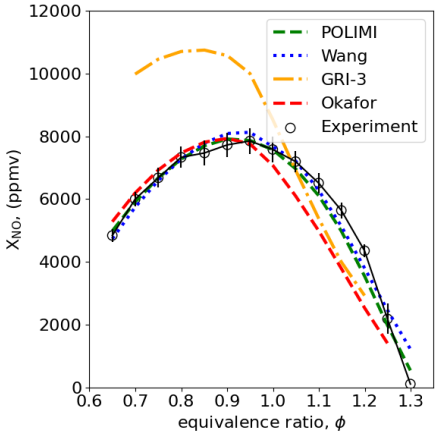

Fig. 1 NO product gas trends with change in equivalence ratio for E_{NH3} = 0.2. Experimental values are from Ref [1].

Figure 2 shows a reaction pathway analysis for the rich region under the same conditions, with hydrocarbon species marked in red, and nitrogen-bound species marked in blue, and cyanide/isocyanides marked in green. Here, the thickness of the arrows was determined by I_R. from Eq. 2 The pathway shows segregation between the NH_3 and CH_4 chemistry routes, but with some interaction between the pathways through the formation of H_2CN and subsequent decomposition of NCO. However, NO-reburn pathways to cyanide and isocyanide species formation and direct amine-hydrocarbon interactions to form methylamines are not considered significant.

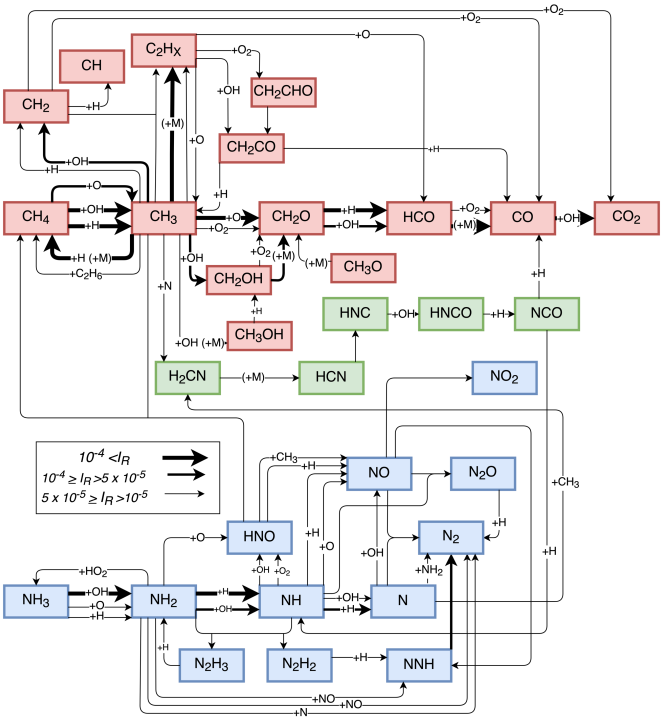

Fig. 2 Integrated ROP pathway analysis for E_{NH3} = 0.2, ϕ = 1.30 using the Wang mechanism.

Since the key interaction points H_2CN and NCO are rarely measured in combustion [19, 20] with the latter being a short-lived radical, other cyanide and isocyanide species can be used as an indicator of interactions between NH_3 and CH_4 chemistry. Figures 3 and 4 provide experimental evidence that the significance of these routes, and especially the role of HCN becomes more significant for E_{NH3} = 0.2 at ϕ > 1.25. The data shows that all mechanisms are able to capture the increase in HCN in the rich region with varying accuracy, with only the Wang mechanism able to capture the increasing HNCO emissions in the rich region. However, further work is needed to measure this species with less uncertainty. It can be deduced from the Wang mechanism predicted emissions and reaction pathway analysis, that similar magnitudes of HNCO are formed as HCN at ϕ = 1.30. However, according to experimental data, significant HCN emissions are measured at ϕ = 1.30, which suggests that further work is needed to understand HCN formation in ammonia/methane flames.

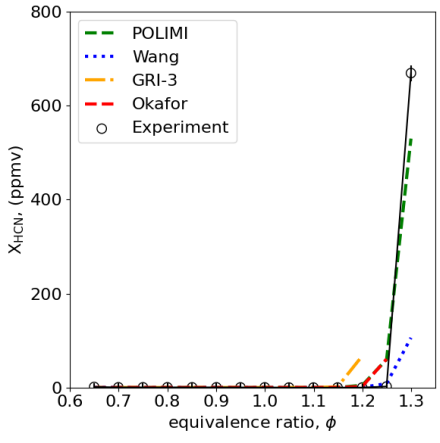

Fig. 3 HCN product gas trends with change in equivalence ratio for E_{NH3} = 0.2. Experimental values are from Ref [1].

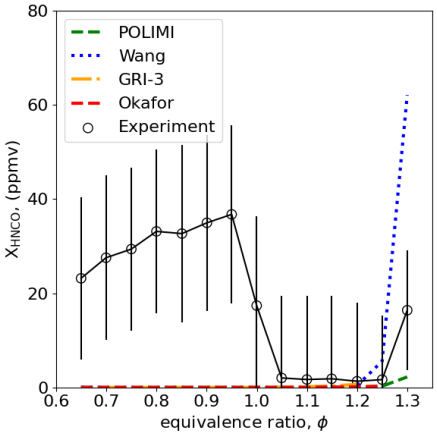

Fig. 4 HNCO product gas trends with change in equivalence ratio for E_{NH3} = 0.2. Experimental values are from Ref [1].

Figure 5 shows the reactions contributing to the integral NO rate of production. The analysis shows that the dominating routes to NO production and consumption are in agreement with literature, mainly through Zel'dovich and HNO and amine (fuel-NO) routes. For the Zel'dovich reactions, $H + NO \rightleftharpoons N + OH$, $N + O_2 \rightleftharpoons NO + O$ are the key production reactions, while $N + NO \rightleftharpoons N_2 + O$ is responsible for the consumption via. the thermal route. HNO reactions with H, CH_3 and OH radicals to form NO produce the remaining production routes for NO. Of these, the $CH_3 + HNO \rightleftharpoons CH_4 + NO$ reaction is can be considered a hydrocarbon-nitrogen chemistry interaction and not included in most NH_3/hydrocarbon mechanisms, including UCSD, Shrestha, GRI3.0, Sun and Okafor. Finally, NH and NH_2 radicals react to consume NO in the post-flame zone. NO-reburn reactions, including NO reactions with CO, HCO, HCCO, HCNO, CH_2 etc. were ranked as minor contributions in the figure.

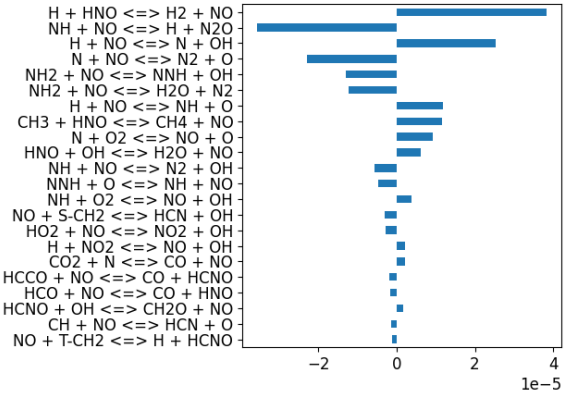

Fig. 5 Integral rate of production contributing directly to NO formation and consumption at E_{NH3} = 0.2 and ϕ = 1.30 (most important reactions listed only).

Figure 6 provides a breakdown by total percentage contribution. Focusing on routes not available in all reaction mechanisms studied, cyanide/isocyanide routes contribute to 2.2%, while the "other nitrogen-hydrocarbon routes" category is responsible for 12.4% of NO production. This "other nitrogen-hydrocarbon routes" category is dominated by the $CH_3 + HNO \rightleftharpoons CH_4 + NO$ reaction. Meanwhile, nine key NO-reburn reactions contribute to a total of 10% of the NO consumption.

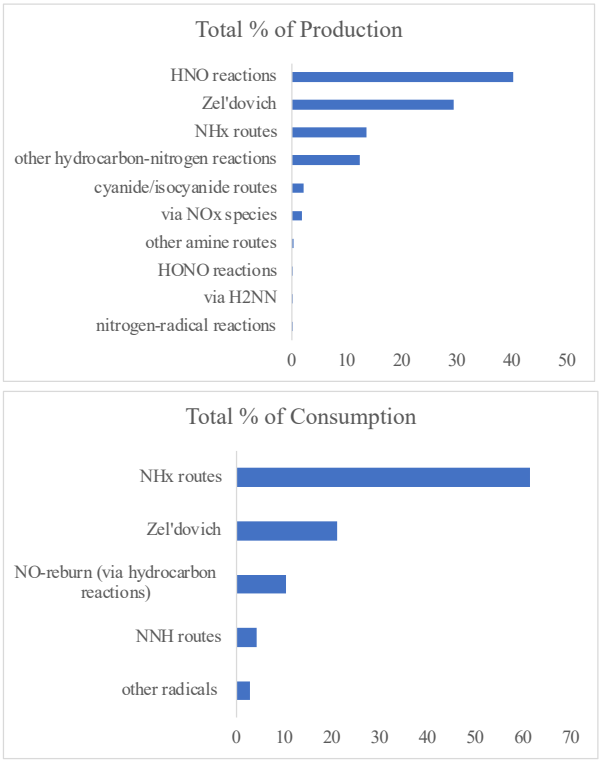

Fig. 6 Reactions category breakdown for NO formation and consumption at E_{NH3} = 0.2 and ϕ= 1.30.

However, NO-reburn reactions and hydrocarbon-nitrogen reactions are not sensitive to the NO emissions value taken at the outlet. Figure 7 shows that of all hydrocarbon reactions, only some involving CH_3, controlling the O, H, OH radical pool are considered significant to NO production. This suggests that in the absence of hydrocarbon-nitrogen interactions, alternative routes to NO will be found, the production/consumption of which continues to be controlled by the O, H, OH radical pool.

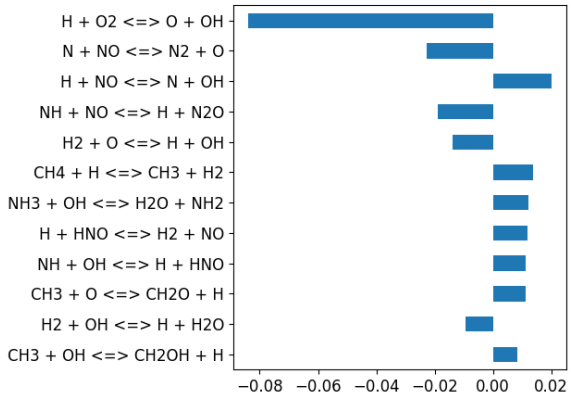

Fig. 7 Sensitivity to NO at the burner stagnation plate at E_{NH3} = 0.2 and ϕ = 1.30.

4. Conclusion

A review of some popular NH_3/CH_4 mechanisms suggests that many do not contain the full hydrocarbon-nitrogen chemistry subsets. The present study found that POLIMI and Wang mechanisms, containing the most complete hydrocarbon-nitrogen chemistry had almost perfect prediction of NO emissions at E_{NH3} = 0.2. A few nitrogen-hydrocarbon reactions, especially CH_3 + HNO ⇌ CH_4 + NO contribute significantly to the formation of NO, though they are neglected from most popular NH_3/CH_4 mechanisms. However, these reactions were not sensitive to the value of NO at the outlet, with reactions either containing NO or controlling the O, OH, H radical pool having the highest sensitivity. This suggests that the superior performance of the detailed mechanisms comes from better fitting reaction constants for key NO, O, H, OH reactions, rather than the inclusion of hydrocarbon-nitrogen chemistry interactions.

Meanwhile NO-reburn reactions contribute to around 10% of the NO consumption, in rich, high methane content blends. However, experimental data shows that the mechanisms tested in the present study were not able to accurately capture trends of HCNO and HCN emissions, which are also the species involved in NO-reburn reactions. Therefore, further experimental data of cyanide and isocyanide species may be necessary to fully understand the role of these species in ammonia/methane chemistry.

Acknowledgment

Part of this study is supported by the collaborative research project of the Institute of Fluid Science, Tohoku University (project code: J23I078).

References

1. Kovaleva, M., Hayakawa, A., Colson, S., Okafor, E. C., Kudo, T., Valera-Medina, A. and Kobayashi, H., Fuel Comms. 100054 (2022).
2. Okafor, E. C., Somarathne, K. D. K. A., Ratthanan, R., Hayakawa, A., Kudo, T., Kurata, O., Iki, N., Tsujimura, T., Furutani, H. and Kobayashi, H., Combust. Flame 211:406–416 (2020).
3. Otomo, J., Koshi, M., Mitsumori, T., Iwasaki, H. and Yamada, K., Int. J Hydrogen Energy 43:3004–3014 (2018).
4. Filipe Ramos, C., Rocha, R. C., Oliveira, PMR., Costa, M. and Bai, X-S., Fuel 254:115693 (2019).
5. Okafor, E., Naito, Y., Colson, S., Ichikawa, A., Kudo, T., Hayakawa, A. and Kobayashi, H., Combust. Flame 187:185–198 (2018).
6. Sun, J., Yang, Q., Zhao, N., Chen, M. and Zheng, H., Fuel 327:124897 (2022).
7. Xiao, H., Valera-Medina, A., Marsh, R. and Bowen, P.J., Numerical study assessing various ammonia/methane reaction models for use under gas turbine conditions. Fuel 196:344–351 (2017).
8. Valera-Medina, A., Marsh, R., Runyon, J., Pugh, D., Beasley, P., Hughes, T. and Bowen, P., Appl Energy 185:1362–1371 (2017).
9. Lin, J-Y., Zhang, S., Zhang, L., Min, Z., Tay, H. and Li, C. Z., HCN and NH3 formation during coal/char gasification in the presence of NO. Environ. Sci. Technol. 44:3719–3723 (2010).
10. Dagaut, P., Glarborg, P. and Alzueta, M. U., Prog. Energy Combust. Sci. 34:1–46 (2008)
11. Takagi, T., Tatsumi, T. and Ogasawara, M., Combust. Flame 35:17–25 (1979).
12. Kristensen, P.G., Glarborg, P. and Dam-Johansen, K., Combust. Flame 107:211–222 (1996).
13. Konnov, A.A., Combust. Flame 156:2093–2105 (2009).
14. Li, W., Li, P., Wang, K., Hu, F. and Liu, L., 27th ICDERS. Beijing, pp. 1–6, 2019.
15. Goodwin, DG., Moffat, HK. and Speth, R. L., available at: https://cantera.org/ Accessed 1 Apr 2016
16. Wang, Z., Han, X., He, Y., Zhu, R., Zhu, Y., Zhou, Z. and Cen, K., Combust. Flame 229:111392 (2021)
17. Smith, G.P., Golden, D.M., Frenklach, M., Moriarty, N.W. and Eiteneer, B., MG GRI-Mech 3.0. In: Gas Research Institute. http://www.me.berkeley.edu/gri_mech/%0A. Accessed 1 Apr 2021
18. William, F. A., Kalyanasundaram, S. and Cattolica, R. J., Chemical-Kinetic Mechanisms for Combustion Applications. http://web.eng.ucsd.edu/mae/groups/combustion/mechanism.html (2012)
19. Bernard, E. J., Strazisar, B. R. and Davis, H. F., Chem. Phys. Lett. 313:461–466 (1999)
20. Lamoureux, N., Mercier, X., Pauwels, J-F. and Desgroux, P., J Phys. Chem. A 115:5346–5353 (2011)
21. Mei, B., Zhang, J., Shi, X., Xi, Z. and Li, Y., Combust. Flame 231:111472 (2021)
22. Shrestha, K. P., Lhuillier, C., Barbosa, A. A., Brequigny, P., Contino, F., Mounaïm-Rousselle, C., Seidel, L. and Mauss, F., 38:2163–2174 (2021)
23. Glarborg, P., Miller, J. A., Ruscic, B. and Klippenstein, S. J., Prog. Energy Combust. Sci. 67:31–68 (2018)
24. Arunthanayothin, S., Stagni, A., Song, Y., Herbinet, O., Faravelli, T. and Battin-Leclerc, F., Proc. Combust. Inst. 38:345–353 (2021)
25. Song, Y., Marrodán, L., Vin, N., Herbinet, O., Assaf, E., Fittschen, C., Stagni, A., Faravelli, T., Alzueta, M. U. and Battin-Leclerc, F., Proc. Combust. Inst. 37:667–675 (2019)